

$^{149}\text{Sm}(n, \alpha)^{146}\text{Nd}$ Cross Sections in the MeV RegionGuohui Zhang,^{1,*} Yu. M. Gledenov,² G. Khuukhenkhuu,³ M. V. Sedysheva,² P. J. Szalanski,⁴ P. E. Koehler,⁵
Yu. N. Voronov,² Jiaming Liu,¹ Xiang Liu,¹ Jinhua Han,¹ and Jinxiang Chen¹¹State Key Laboratory of Nuclear Physics and Technology, Institute of Heavy Ion Physics, Peking University, Beijing 100871, China²Frank Laboratory of Neutron Physics, JINR, Dubna 141980, Russia³Nuclear research Centre, National University of Mongolia, Ulaanbaatar, Mongolia⁴University of Lodz, Institute of Physics, Lodz, Poland⁵Physics Division, Oak Ridge National Laboratory, Oak Ridge, Tennessee 37831, USA

(Received 21 August 2011; published 14 December 2011)

We have measured the $^{149}\text{Sm}(n, \alpha)^{146}\text{Nd}$ cross section at 4.5, 5.0, 5.5, 6.0, and 6.5 MeV. Measurements were performed at the 4.5 MV Van de Graaff accelerator of Peking University with monoenergetic neutrons produced via the $^2\text{H}(d, n)^3\text{He}$ reaction using a deuterium gas target. Alpha particles were detected with a double-section gridded ionization chamber having two back-to-back $^{149}\text{Sm}_2\text{O}_3$ samples attached to the common cathode. Absolute neutron flux was measured using a small ^{238}U fission chamber and monitored by a BF_3 long counter. These are the first reported cross sections for this reaction at these energies, except at 6.0 eV, where our new data are in good agreement with our earlier result. The present results help to much better constrain the $^{149}\text{Sm}(n, \alpha)^{146}\text{Nd}$ cross section in a region where its energy dependence is changing fairly rapidly and there are large differences between evaluated nuclear data libraries.

DOI: 10.1103/PhysRevLett.107.252502

PACS numbers: 28.20.-v, 24.10.-i, 25.40.-h

The $^{149}\text{Sm}(n, \alpha)^{146}\text{Nd}$ cross section is of interest for both basic and applied nuclear physics. For example, in nuclear astrophysics, measurements of this cross section can be used to improve reaction rates used in explosive nucleosynthesis calculations [1]. Also, because ^{149}Sm is a fission-product nucleus with relatively high yield, the $^{149}\text{Sm}(n, \alpha)^{146}\text{Nd}$ cross section is needed for nuclear-energy applications, and hence it has been evaluated and incorporated into nuclear data libraries such as ENFD/B, ROSFOND, BROND, JEFF, JENDL, CENDL, and TENDL [2]. Because ^{149}Sm is a neutron poison in nuclear reactors, its (n, α) cross section has been measured at thermal, epithermal, as well as 14 MeV neutron energy regions [3–7]. However, in the MeV neutron energy range, there has been only one previously reported measurement [8], and none of the available nuclear data libraries (which were compiled before this measurement) agreed with this datum to within the measurement uncertainty. Because of the lack of data, evaluated nuclear data libraries rely heavily on nuclear model calculations in this energy region, and hence there are large differences between the various evaluations. Furthermore, all evaluations indicate that the cross section is changing rapidly in this energy region. For these reasons, new $^{149}\text{Sm}(n, \alpha)^{146}\text{Nd}$ cross-section measurements are necessary at MeV energies.

Because the residual nucleus ^{146}Nd is stable, the commonly used activation method is not applicable. Measurements are further limited in this energy region by the small cross section, potentially large backgrounds, and low neutron source intensity.

Our previous measurement at 6.0 MeV [8] required 63 h of beam time despite the fact that we used two large-area

samples and a detector with nearly 100% efficiency over 4π solid angle. To make measurements at lower energies where the cross section is even smaller would have required prohibitively long beam time. Therefore, we used thicker samples in our new measurements, which required larger corrections for α -particle straggling and absorption. To check these larger corrections, our new measurements included one at 6.0 MeV, which could be compared to our previous result. We found a good agreement between our new and previous cross sections, thus verifying the accuracy of our technique.

Important components of the apparatus and the relevant geometric parameters are shown in Figs. 1 and 2, respectively. There were two important differences compared to Ref. [8]. First, (approximately 4 times) thicker $^{149}\text{Sm}_2\text{O}_3$ samples were employed to reduce total beam time. Second, the distance from the small fission chamber to the neutron source was increased to improve the accuracy of the neutron flux determination.

Both forward and backward ^{149}Sm samples were prepared by the sedimentation technique. Relevant sample

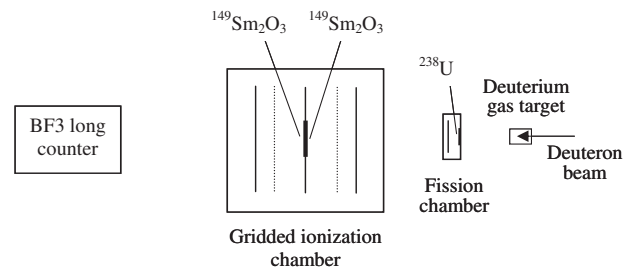


FIG. 1. Experimental apparatus.

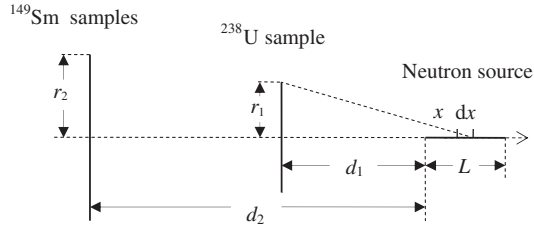


FIG. 2. Geometry of the neutron source and the ^{238}U and ^{149}Sm samples (not to scale).

parameters are listed in Table I. The thickness of each $^{149}\text{Sm}_2\text{O}_3$ sample was determined by weight, and the number of the ^{149}Sm atoms was determined from the chemical and isotopic parameters given in Table I. The number of the ^{238}U nuclei in the monitor sample was measured by counting the α activity using two detectors: the gridded ionization chamber and a silicon surface barrier detector, and the results are in agreement within measurement uncertainties.

The two $^{149}\text{Sm}_2\text{O}_3$ samples were mounted back to back on the common cathode of the double-section gridded ionization chamber, details of which can be found in Ref. [9]. Two retractable α sources inside the gridded ionization chamber were used for energy calibration and adjustment of the data acquisition system. Alpha events from the $^{149}\text{Sm}(n, \alpha)^{146}\text{Nd}$ reaction were detected independently and simultaneously in both forward (0° – 90°) and backward (90° – 180°) directions.

Neutrons were produced through the $^2\text{H}(d, n)^3\text{He}$ reaction using a deuterium gas target bombarded by a deuteron beam, which was accelerated by the 4.5 MV Van de Graaff accelerator of Peking University. The beam current was about $3.0 \mu\text{A}$ throughout the measurement. Details of the gas target can also be found in Ref. [9]. Neutron energies, energy spreads, and measurement durations are listed in Table II. Total measurement duration for the five energies was about 97 h.

The neutron flux was monitored by the BF_3 long counter shown in Fig. 1, and absolute neutron flux was determined using the small ^{238}U fission chamber by counting the fission fragments. Parameters of the ^{238}U sample are given in Table I.

TABLE II. Neutron energies, energy spreads, measurement durations, and G values (see the text) of the present work.

E_n (MeV)	Energy spread 1σ (MeV)	Measurement duration (h)	G value
4.5	0.19	26	49.66
5.0	0.16	24	49.20
5.5	0.14	21	48.78
6.0	0.12	15	48.40
6.5	0.10	11	48.02

The length of the deuterium gas cell was 1.80 cm. Distances from the ^{238}U and ^{149}Sm samples to the near end of the gas cell were 3.15 and 27.7 cm, respectively.

Cathode-anode coincident two-dimensional spectra of the gridded ionization chamber were recorded for both forward and backward α events from the $^{149}\text{Sm}(n, \alpha)^{146}\text{Nd}$ reaction. The anode spectrum of the ^{238}U fission chamber was recorded, too.

The cross section $\sigma_{n,\alpha}$ of the $^{149}\text{Sm}(n, \alpha)^{146}\text{Nd}$ reaction can be determined by the following equation:

$$\sigma_{n,\alpha} = G \sigma_{n,f} \frac{N_\alpha}{N_f} \frac{N_{238\text{U}}}{N_{149\text{Sm}}}, \quad (1)$$

where $\sigma_{n,f}$ is the standard cross section of the $^{238}\text{U}(n, f)$ reaction taken from ENDF/B-VII.0 [2], N_α and N_f are numbers of the α and fission events from the $^{149}\text{Sm}(n, \alpha)^{146}\text{Nd}$ and $^{238}\text{U}(n, f)$ reactions, respectively, $N_{238\text{U}}$ and $N_{149\text{Sm}}$ are the numbers of ^{238}U and ^{149}Sm atoms in the samples, respectively, and G is the ratio of the average neutron flux densities through the ^{238}U and $^{149}\text{Sm}_2\text{O}_3$ samples.

The value of G was determined by the geometry of the neutron source, ^{238}U and ^{149}Sm samples (see Fig. 2), as well as the angular distribution [10] of the source neutrons using the following expression:

$$G = \frac{\int_0^L dx \int_0^{2\pi} d\varphi \int_0^{\arctan[r_1/(d_1+x)]} \sin\theta \sigma(\theta) d\theta \pi r_2^2}{\int_0^L dx \int_0^{2\pi} d\varphi \int_0^{\arctan[r_2/(d_2+x)]} \sin\theta \sigma(\theta) d\theta \pi r_1^2}, \quad (2)$$

where L is the length of the deuterium target gas cell, r_1 , r_2 and d_1 , d_2 are the radii of the ^{238}U and ^{149}Sm samples and the distances from the near end of the gas cell to each of

TABLE I. Description of the samples.

	^{149}Sm samples	^{238}U sample
Sample material	$^{149}\text{Sm}_2\text{O}_3$ purity 99.96%	$^{238}\text{U}_3\text{O}_8$
Isotopic enrichment	^{149}Sm 94.6%	^{238}U 99.997%
Sample thickness	4.72 ^a and 3.97 ^b mg/cm ²	0.174 mg/cm ² (^{238}U only)
Sample diameter	11.5 cm	2.0 cm
Backing material and thickness	Aluminum 0.10 mm	Stainless steel 0.30 mm

^aForward sample.

^bBackward sample.

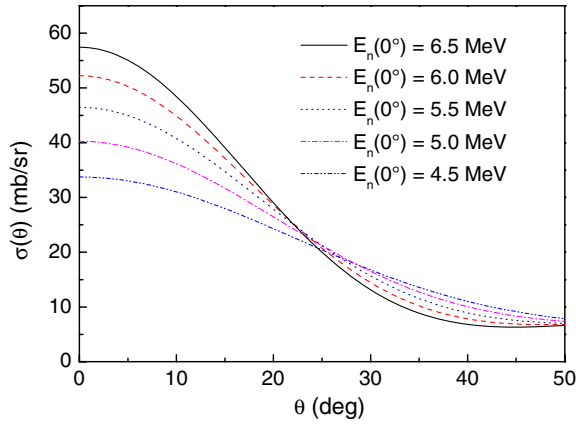


FIG. 3 (color online). Differential cross sections of the ${}^2\text{H}(d, n){}^3\text{He}$ reaction [10].

them, respectively (Fig. 2), and $\sigma(\theta)$ is the differential cross section of the ${}^2\text{H}(d, n){}^3\text{He}$ reaction (Fig. 3).

Relevant distances during the measurements were $r_1 = 1.0$ cm, $r_2 = 5.75$ cm, $d_1 = 3.15$, $d_2 = 27.7$ cm, and $L = 1.8$ cm (Fig. 2). Calculated G values are listed in Table II with uncertainty 2.5%. They are slightly smaller than $[(d_2 + L/2)/(d_1 + L/2)]^2 = 49.87$ and the uncertainty in G is dominated by the uncertainty of d_1 , as d_1 is much smaller than d_2 . Thus, a relatively small increase in d_1 can effectively improve the accuracy of the G values.

The calculated G values were compared with measurements made using one ${}^{238}\text{U}$ sample in the fission chamber and another ${}^{238}\text{U}$ sample attached to the common cathode of the gridded ionization chamber. The measured and calculated G values agreed to within the uncertainties [11].

As explained in Refs. [8,12], kinematics curves defining the expected location of events from the ${}^{149}\text{Sm}(n, \alpha){}^{146}\text{Nd}$ reaction in the anode-cathode coincidence spectra were used to reduce backgrounds. We obtained the α spectrum (as shown in Fig. 4 for the incident energy of 5.0 MeV) by projecting events between the 0° and 90° curves (or 180° and 90° curves) in the anode-cathode coincidence spectra for the forward (or backward) section of the ion chamber onto the anode axis.

Although higher- Z krypton rather than the more usual argon was used as the main gas in the ion chamber, as can be seen in Fig. 4 the background was still relatively high at low α energies. To minimize the effects of this background, a threshold was set, and the number of α counts above this threshold was obtained as $N_{\alpha\text{det}}$. If the fraction of α events below threshold (including those emitted at large angles that were absorbed by the samples) in total α events is denoted by R , then the true number of α events N_α from the ${}^{149}\text{Sm}(n, \alpha){}^{146}\text{Nd}$ reaction is given by

$$N_\alpha = \frac{N_{\alpha\text{det}}}{1 - R}. \quad (3)$$

The fraction of events below threshold was calculated via Monte Carlo simulations using the code SRIM [13] to

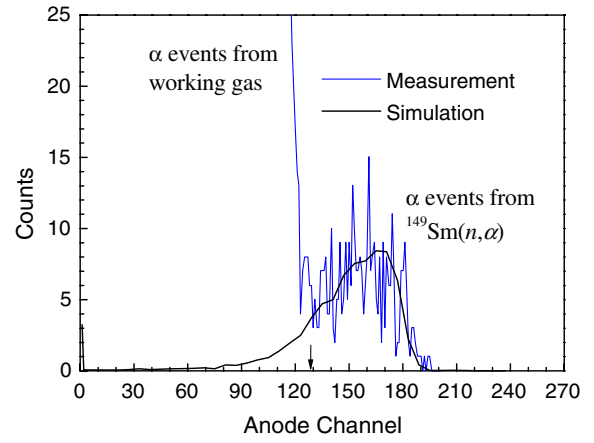


FIG. 4 (color online). Projected α spectrum measured with the forward section of the ion chamber at $E_n = 5.0$ MeV compared with SRIM simulation (the arrow indicates threshold channel of 129).

predict the α straggling and absorption in the samples. The code TALYS-1.0 [14] was used to predict the needed angular and energy distributions of the emitted α particles.

Major sources of uncertainty for $N_{\alpha\text{det}}$ were counting statistics (4.5%–9%) and threshold location (6%). Total uncertainty in $N_{\alpha\text{det}}$ was between 7.5% and 11%.

Values of R varied from 20% to 45% depending on the original α emission spectra, the thresholds, and thicknesses of the samples. The uncertainty in R was estimated to be 20%–25%. Therefore, the total uncertainty in N_α was about 17%.

Fission counts N_f were obtained from the anode spectrum from the small ${}^{238}\text{U}$ fission chamber, as shown in Fig. 5.

Once N_α and N_f were obtained, forward and backward cross sections for each energy point were calculated using Eq. (1). Subsequently, total (n, α) cross sections and forward/backward ratios were calculated, and are given in Table III (in the laboratory reference system).

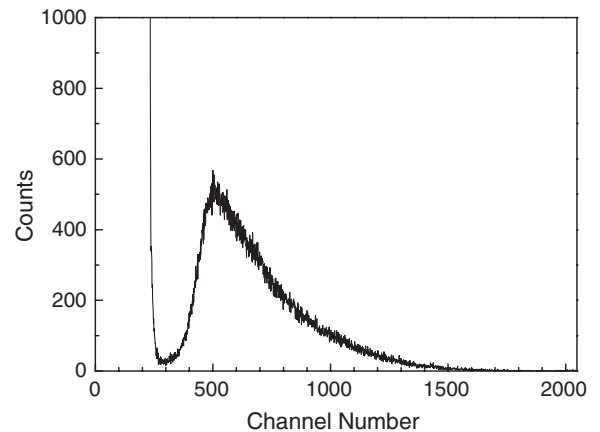


FIG. 5. Fission spectrum from the small ${}^{238}\text{U}$ fission chamber at $E_n = 5.0$ MeV.

TABLE III. Measured $^{149}\text{Sm}(n, \alpha)^{146}\text{Nd}$ cross sections and forward/backward ratios (in the laboratory reference system) from the present work compared with model calculations (TALYS-1.0, $0.5r_D$).

E_n (MeV)	$\sigma_{n,\alpha}$ (mb)		Forward/backward ratio	
	Measured	Calculated	Measured	Calculated
4.5	0.049 ± 0.009	0.0274	1.4 ± 0.35	1.39
5.0	0.057 ± 0.010	0.0462	1.6 ± 0.4	1.51
5.5	0.084 ± 0.015	0.0803	1.9 ± 0.5	1.62
6.0	0.10 ± 0.02	0.142	2.2 ± 0.6	1.72
6.5	0.19 ± 0.03	0.247	2.7 ± 0.7	1.81

A total uncertainty in the cross sections of 18% was obtained by adding in quadrature uncertainties in the number of α events N_α (17%), fission counts N_f (2.5%), ratio of neutron fluxes G (2.5%), ^{238}U fission cross section (1%), and the number of ^{149}Sm (1.5%) and ^{238}U (1.3%) atoms in the samples.

Small corrections were made for the neutron flux attenuation in the 2-mm-thick aluminum wall of the chamber and the 0.2-mm-thick aluminum backing of the two samples using the total neutron cross section of aluminum in ENDF/B-VII.0 [2].

The code TALYS-1.0 [14] was used to calculate theoretical cross sections and forward/backward ratios. Parameters of the α -optical-model potential were adjusted in an attempt to obtain a good agreement with experimental results. As can be seen in Table III and Fig. 6, a good agreement between statistical model calculations and the measured cross sections from thermal to MeV energies could be achieved by modest adjustment of the parameter (r_D was adjusted to half of its default value). However, we could find no combination of parameters that would reproduce the data of Augustyniak *et al.* [7] near 14 MeV.

Our new cross sections are compared with previous measurements, evaluations, and TALYS calculations in

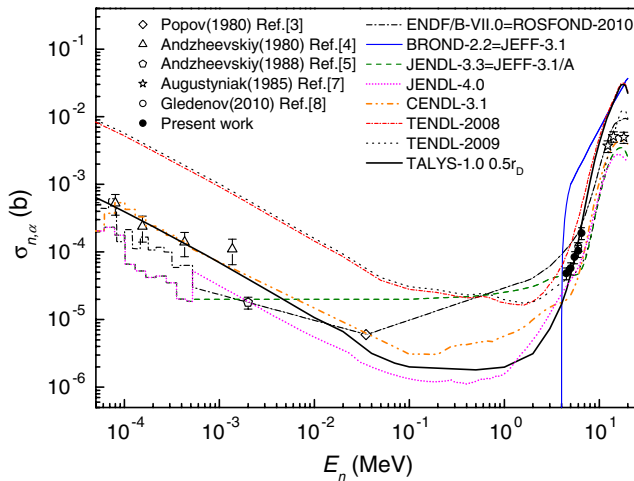


FIG. 6 (color online). Present cross sections of the $^{149}\text{Sm}(n, \alpha)^{146}\text{Nd}$ reaction compared with nuclear data library evaluations and TALYS-1.0 code calculations.

Fig. 6, in which one can see that very large differences exist between the evaluations. For example, at 5.0 MeV the largest evaluation is more than 40 times larger than the smallest. None of the evaluations agree with our results within the uncertainties. Our new data are in good agreement with our previous measurement at 6.0 MeV [8], although our new samples were much thicker, lending confidence to our experimental techniques and data-correction procedures.

In summary, cross sections of the $^{149}\text{Sm}(n, \alpha)^{146}\text{Nd}$ reaction were measured for the first time at 4.5, 5.0, 5.5, and 6.5 MeV neutron energy points. Measurement at 6.0 MeV was repeated with thicker samples, and the consistency was achieved. Small cross section as $50 \mu\text{b}$ was obtained using our measurement facility. Our results are different from all existing evaluations of nuclear data libraries. Model calculations using the TALYS-1.0 code are performed, and a good agreement is achieved between measurements and calculations from thermal to MeV energies. The present results help to much better constrain the $^{149}\text{Sm}(n, \alpha)^{146}\text{Nd}$ cross section in the MeV energy region where its energy dependence is changing fairly rapidly and there are large differences between evaluated nuclear data libraries. New measurements in the 12–20 MeV region to check the results of Augustyniak *et al.* [7] are suggested.

Two anonymous reviewers are acknowledged for their insightful comments that improved this Letter. The authors are indebted to the operation team of the 4.5 MV Van de Graaff accelerator of Peking University. This work was financially supported by the National Natural Science Foundation of China (10875006), the Science and Technology on Nuclear Data Laboratory, China Nuclear Data Center, the Russian Foundation for Basic Research (RFBR-NSFC 07-02-92104), and the Office of Nuclear Physics of the U.S. Department of Energy under Contract No. DEAC05-00OR22725 with UT-Battelle, LLC.

*Corresponding author.

guohuizhang@pku.edu.cn

[1] Yu. M. Gledenov, P. E. Koehler, J. Andrzejewski, and K. H. Guber, *Phys. Rev. C* **62**, 042801(R) (2000).

- [2] Evaluated Nuclear Data File (ENDF), Database Version of February 08, 2011, <http://www-nds.iaea.org/exfor/endl.htm>.
- [3] Yu. P. Popov, V. I. Salackij, and G. Khuukhenkhuu, *Yad. Fiz.* **32**, 893 (1980) [*Sov. J. Nucl. Phys.* **32**, 459 (1980)].
- [4] Yu. Andzheevskiy, V. K. Tkhan, V. A. Vtyurin, A. Koreyvo, Yu. P. Popov, and M. Stempinsky, *Yad. Fiz.* **32**, 1496 (1980) [*Sov. J. Nucl. Phys.* **32**, 774 (1980)].
- [5] Yu. Andzheevskiy, V. P. Vertebnyi, V. K. Tkhan, V. A. Vtyurin, A. L. Kirilyuk, and Yu. P. Popov, *Yad. Fiz.* **48**, 20 (1988) [*Sov. J. Nucl. Phys.* **48**, 12 (1988)].
- [6] K. Beg and R. D. Macfarlane, *Bull. Am. Phys. Soc.* **10**, 724 (1965).
- [7] W. Augustyniak, L. Glowacka, M. Jaskola, J. Turkiewicz, L. Zemlo, J. Dalmas, E. Gadioli, and E. Gadioli Erba, *Nuovo Cimento Soc. Ital. Fis. A* **85**, 217 (1985).
- [8] Yu. M. Gledenov, G. Zhang, G. Khuukhenkhuu, M. V. Sedysheva, P. J. Szalanski, P. E. Koehler, J. Liu, H. Wu, X. Liu, and J. Chen, *Phys. Rev. C* **82**, 014601 (2010).
- [9] Yu. M. Gledenov, M. V. Sedysheva, V. A. Stolupin, Guohui Zhang, Jiaguo Zhang, Hao Wu, Jiaming Liu, Jinxiang Chen, G. Khuukhenkhuu, P. E. Koehler, and P. J. Szalanski, *Phys. Rev. C* **80**, 044602 (2009).
- [10] M. Drosog, Report No. IAEA-NDS-87, 2003.
- [11] G. Zhang, X. Liu, Z. Gao, H. Wu, and J. Liu, “Analysis and comparison of monoenergetic fast neutron flux determination using ^{238}U samples at different positions with respect to the neutron source” (to be published).
- [12] N. Ito, M. Baba, S. Matsuyama, I. Matsuyama, and N. Hirakawa, *Nucl. Instrum. Methods Phys. Res., Sect. A* **337**, 474 (1994).
- [13] SRIM, <http://www.srim.org/#SRIM>, 2010.
- [14] A. J. Koning, S. Hilaire, and M. C. Duijvestijn, in *Proceedings of the International Conference on Nuclear Data for Science and Technology, Nice, France, 2007*, edited by O. Bersillon, F. Gunsing, E. Bauge, R. Jacqmin, and Sylvie Leray (EDP Sciences, Les Ulis, France, 2008), p. 211.